2. SUPERSONIC BEAM SOURCES

Michael D. Morse
Department of Chemistry, University of Utah
Salt Lake City, Utah

2.1 Introduction

Within the past 20 years, supersonic molecular beams have been put to ever-increasing use as a tool of atomic and molecular physics. In particular, supersonic expansions provide a means of preparing a molecular beam with a well-defined kinetic energy, which is particularly useful for crossed–beam and beam–surface scattering experiments. In addition, the nearly complete conversion of enthalpy to directed mass flow leads to the production of molecular beams with extremely low internal temperatures, allowing weakly bound van der Waals complexes to be prepared and spectroscopically characterized. The low internal temperatures achieved in supersonic expansions also lead to a dramatic reduction in spectral congestion and have permitted interpretable spectra to be recorded for many species which would otherwise be impossible to investigate. Clever techniques have allowed radicals, refractory species, and ions to be investigated as well. Most recently, the dramatic cooling achievable in a supersonic expansion has permitted the van der Waals molecule $^4He_2$ to be produced and detected [1], a remarkable achievement given that the ground state is predicted to be only bound by 0.0006 to 0.0011 cm^{-1} (0.8 to 1.6 mK) [2].

Here we review the salient features of supersonic expansions and their use in chemical physics.

2.2 Effusive Beams

The expansion of a high-pressure gas from a reservoir into vacuum can occur via two physically distinct limiting cases, depending on the relationship between the mean free path of the gas molecules in the reservoir, λ_0, and the diameter (or width), D, of the expansion orifice (or slit). As these characteristic dimensions approach the limit $\lambda_0 \gg D$, the number of collisions suffered by a molecule as it leaves the reservoir approaches zero, and an effusive beam is generated with a velocity distribution of

$$P(v)dv = \frac{m^2}{2(RT_0)^2} v^3 \exp\left[- \frac{mv^2}{2RT_0} \right] dv, \tag{2.1}$$

EXPERIMENTAL METHODS IN THE PHYSICAL SCIENCES
Vol. 29B

where m is the molar mass of the molecule, R the gas constant, and T_0 the temperature of the reservoir [3]. This distribution is determined by T_0 and m, but is otherwise independent of details such as the pressure in the reservoir and the presence of other species effusing from the expansion orifice. Because no collisions occur during the expansion process, effusive beams provide a means of probing the conditions inside the reservoir at an elevated temperature and have been usefully combined with mass spectrometric methods to evaluate equilibrium constants and provide thermochemical data for gas-phase reactions at elevated temperatures. This is the basis for the field of Knudsen effusion mass spectrometry [4]. Effusive beams are discussed more thoroughly in the preceding chapter, and the reader interested in these topics is referred there for more details [3].

2.3 Supersonic Expansions from Circular Nozzles (Axisymmetric Jets)

2.3.1 The Idealized Continuum Model

In the limit of $D \gg \lambda_0$, molecules escaping from the reservoir suffer many collisions during the expansion process, which is then governed by gas dynamic equations similar to those used in the design of aircraft [5]. The theory in its most basic form was first worked out in 1951 [6], and experimental proof of the fundamental principles was provided shortly thereafter [7, 8]. At high source pressures, the effects of gas viscosity and heat transfer may be neglected, and the gas flow may be treated as an adiabatic, isentropic expansion. The adiabatic assumption leads to the conservation of the sum of the enthalpy and the kinetic energy of directed mass flow as the gas expands into vacuum [5], so that

$$H(x) + \tfrac{1}{2}mu(x)^2 = \text{constant}, \tag{2.2}$$

where $H(x)$ is the molar enthalpy of the gas at position x from the point of expansion and $u(x)$ is the average flow velocity at this position. This equation limits the ultimate flow velocity, u, to the value

$$u_{\max} = \sqrt{\frac{2H(T_0)}{m}}, \tag{2.3}$$

where $H(T_0)$ is the molar enthalpy of the gas at the temperature of the source reservoir, T_0. For calorically perfect gases which have a constant-pressure molar heat capacity, C_p, that is independent of temperature, $H(T)$ is given as $C_p T$, and the ultimate flow velocity becomes

$$u_{\max} = \sqrt{\frac{2C_p T_0}{m}}. \tag{2.4}$$

For an ideal monatomic gas, $C_p = \frac{5}{2}R$, and Eq. (2.4) predicts terminal velocities of 1.77×10^5, 7.86×10^4, 5.59×10^4, 3.86×10^4, and 3.08×10^4 cm/s for He, Ne, Ar, Kr, and Xe, respectively, expanding from a reservoir at 300 K. In practice, velocities closely approaching these values are readily achieved, particularly for He, Ne, and Ar, which are much less subject to condensation and clustering than their heavier analogues. In general, the assumption of an isentropic expansion is reasonably well validated by measurements of local temperatures at varying distances downstream from the point of expansion [10].

For a calorically perfect ideal gas [defined by the relationships $dH = C_p dT$ (with C_p independent of temperature) and the ideal gas law, $p = \rho kT$], adiabatic isentropic expansion from a reservoir at conditions (p_0, T_0, ρ_0) to final conditions (p_1, T_1, ρ_1) then gives

$$\frac{T_1}{T_0} = \left(\frac{p_1}{p_0}\right)^{(\gamma-1)/\gamma}; \qquad \frac{\rho_1}{\rho_0} = \left(\frac{p_1}{p_0}\right)^{1/\gamma}; \qquad \text{and} \quad \frac{\rho_1}{\rho_0} = \left(\frac{T_1}{T_0}\right)^{1/(\gamma-1)}, \tag{2.5}$$

where ρ is the density of the gas and γ is the heat capacity ratio C_p/C_v, equal to $1.666\bar{6}$ (5/3) for monatomic gases, 1.4 (7/5) for diatomic gases ignoring vibration, and 1.2857 (9/7) for diatomic gases at high temperatures where vibration contributes Nk to the heat capacity. These equations imply that an expansion carried out with a large pressure ratio will lead to a large reduction in temperature.

The propagation of sound in a gas is also an example of an adiabatic, nearly isentropic process [5], and the speed of sound, a, in an ideal gas is given as

$$a(T) = \sqrt{\frac{\gamma RT}{m}}. \tag{2.6}$$

The Mach number, $M(x)$, is then defined as the ratio of the average flow velocity of the expanding gas at position x, $u(x)$, to the local speed of sound of the gas, $a(x)$, i.e., $M(x) = u(x)/a(x)$. The substantial cooling associated with supersonic expansion reduces the local speed of sound of the expanding gas tremendously, while the average flow velocity, $u(x)$, increases as random motion is converted into directed mass flow (but never exceeding u_{max}, as discussed earlier). The expansion is said to become supersonic when the ratio $u(x)/a(x)$ (or the Mach number, $M(x)$), increases beyond unity. Experimentally, it is not difficult to achieve Mach numbers of 20 or greater in a supersonic expansion.

Combining Eqs. (2.2), (2.5), and (2.6), it is possible to express the temperature, pressure, and density ratios in terms of the Mach number, $M(x)$, as

$$\frac{T(x)}{T_0} = W^{-1}; \qquad \frac{p(x)}{p_0} = W^{-\gamma/(\gamma-1)}; \qquad \frac{\rho(x)}{\rho_0} = W^{-1/(\gamma-1)}, \tag{2.7}$$

where

$$W \equiv 1 + \frac{\gamma - 1}{2} M(x)^2.$$

Finally, the functional dependence of the Mach number on downstream distance, x, has been calculated using the method of characteristics [11], and an accurate fitting formula has been developed [12], providing

$$M(x) = A\left(\frac{x - x_0}{D}\right)^{\gamma-1} - \frac{1}{2}\frac{[(\gamma + 1)/(\gamma - 1)]}{A[(x - x_0)/D]^{\gamma-1}}, \tag{2.8}$$

where D is the orifice diameter, and x_0/D and A depend on γ as given in Table I. The translational temperature predicted from Eqs. (2.7) and (2.8) is displayed in Figure 1 for the expansion of an ideal gas, as a function of the distance from the point of expansion, measured in units of the nozzle diameter, x/D.

Using Eq. (2.8) in combination with Eq. (2.7), one obtains asymptotic expressions for the temperature, pressure, and density ratios at large distances x/D as

$$\begin{aligned}
\frac{T(x)}{T_0} &= B\left(\frac{x - x_0}{D}\right)^{-2(\gamma-1)}; \\
\frac{p(x)}{p_0} &= C\left(\frac{x - x_0}{D}\right)^{-2\gamma}; \\
\frac{\rho(x)}{\rho_0} &= F\left(\frac{x - x_0}{D}\right)^{-2},
\end{aligned} \tag{2.9}$$

where B, C, and F are constants determined from A and γ. Note that $\rho(x)/\rho_0$ displays the inverse-square law decrease expected in the limiting region where the molecules expand along straight but diverging streamlines.

TABLE I. Values of Parameters Used in Eqs. (2.8) and (2.13)

γ	x_0/D	A	G
1.66$\bar{6}$ (5/3)	0.075	3.26	2.03
1.40 (7/5)	0.40	3.65	2.48
1.30	0.70	3.90	2.80
1.286 (9/7)	0.85	3.96	2.85
1.20	1.00	4.29	3.38
1.10	1.60	5.25	4.75
1.05	1.80	6.44	7.04

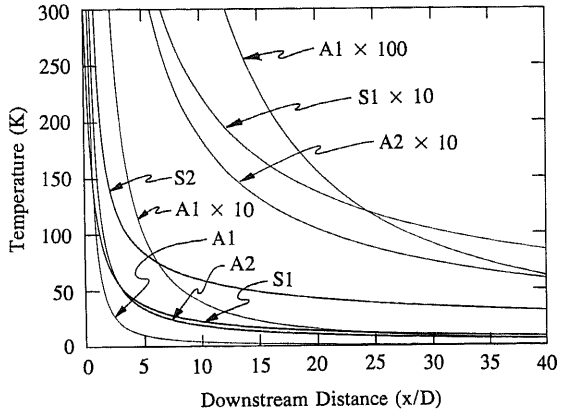

FIG. 1. Translational temperatures achieved in idealized continuum flow expansions. Results for axisymmetric jets with $\gamma = 1.666$ (5/3) (monatomic gases), labeled by A1, and for axisymmetric jets with $\gamma = 1.400$ (7/5) (diatomic gases with frozen vibrations), labeled by A2, are given as functions of the downstream distance, x/D. The corresponding results for slit nozzle expansions are labeled S1 and S2, respectively. For the A1, A2, and S1 examples, the function is plotted with the ordinate expanded by a factor of 10 or 100, indicated by A1 × 10, etc.

The distribution of molecular velocities, $P(v)$, can also be derived and is given as

$$P(v) \propto v^3 \exp\left[-\frac{m(v-u(x))^2}{2RT(x)}\right], \tag{2.10}$$

where $T(x)$ and $u(x)$ represent the local temperature and average flow velocity in the expansion, with $T(x)$ calculated from Eqs. (2.7) and (2.8). The average flow velocity is calculated through Eq. (2.2), which provides

$$u(x) = \sqrt{2[H(T_0) - H(T(x))]/m}, \tag{2.11}$$

where H is again the molar enthalpy as a function of temperature. Normalized velocity distributions are displayed in Figure 2 for a Maxwell–Boltzmann distribution at 300 K, along with the results of Eq. (2.1) for an effusive beam with source temperature 300 K and the results of Eq. (2.1) for a supersonically expanded beam reaching Mach numbers of 2, 5, 10, 20, and 30 from a 300 K source. In all cases the gas is assumed to be ^{4}He; for other species the velocity distribution scales according to $m^{-1/2}$.

2.3.2 Departures from the Idealized Continuum Model

The idealized continuum model assumes that collisions occur with sufficient frequency for equilibrium to be maintained throughout the expansion process. At

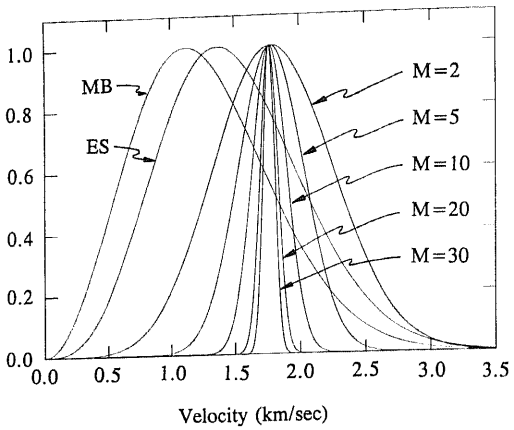

FIG. 2. Velocity distributions obtained for ^{4}He expansions from a reservoir at 300 K, normalized to a peak value of unity. The Maxwell–Boltzmann distribution of atomic speeds in the reservoir is labeled MB, the distribution of velocities along the centerline of an effusive source is labeled ES, and the velocity distributions along the centerline of an expansion attaining Mach numbers of 2, 5, 10, 20, and 30 are indicated by the designations M = 2, M = 5, etc.

some point in the expansion, however, the collision frequency drops to such a low level that a particular degree of freedom may fall out of equilibrium. This is the beginning of the transition from continuum flow to free molecular flow, which ultimately leads to gas phase molecules isolated in a (nearly) collision-free environment. Generally, rotational relaxation occurs more readily than vibrational relaxation, and translational energy exchange occurs even more easily than rotational relaxation. For these reasons, it is typically the vibrational degrees of freedom which fall out of equilibrium first, followed by the rotational degrees of freedom. Finally, collisions become so infrequent that translational equilibration ceases, and the continuum model becomes invalid.

Knowing the distribution of velocities, $P(v)$, and the density, ρ, at various positions downstream, and making some simple assumptions concerning the effectiveness of collisional energy transfer, it can be shown that a real supersonic expansion will reach a terminal Mach number, M_T, beyond which no further cooling occurs [10]. M_T has been shown to depend on a constant depending only on γ (given by G, and listed in Table I), λ_0/D, and a collisional effectiveness parameter, ε, which denotes the maximum fractional change in the mean random velocity per collision, giving [10, 13]

$$M_T = G\left(\frac{\lambda_0}{D\varepsilon}\right)^{-(\gamma-1)/\gamma}. \tag{2.12}$$

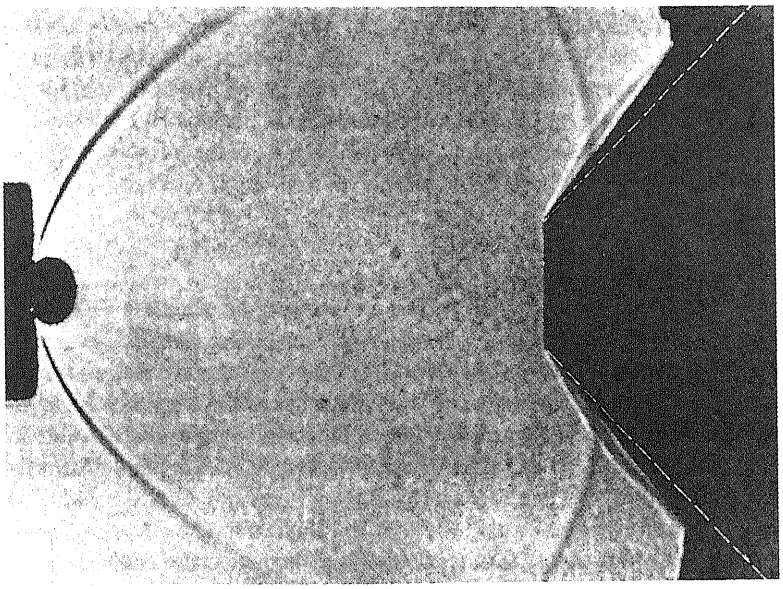

FIG. 3. Shadowgram of a freely expanding jet of N_2 emerging from a reservoir held at a pressure of 100 atm into a vacuum chamber maintained at 50 torr. The barrel shock is clearly visible, as is the terminal shock wave (Mach shock wave). A skimmer is used to transmit the central portion of the expansion into a second chamber, and an attached shock wave is visible on the outside of the skimmer. Reprinted, with permission, from reference [16].

Assuming a single component gas in the source reservoir, this may be written as

$$M_T = G(\sqrt{2}\sigma\rho_0 D\varepsilon)^{(\gamma-1)/\gamma}, \tag{2.13}$$

where σ is the collision cross section and ρ_0 is the number density of gas molecules in the source reservoir. Experiments using argon have demonstrated that M_T is given by $M_T = 1.17\ (\sqrt{2}\sigma\rho_0 D)^{0.4}$, where the exponent 0.4 follows from Eq. (2.13) with $\gamma = 5/3$. M_T is related to $\rho_0 D$ (or at fixed source temperature, to $p_0 D$), so that if a greater degree of cooling is desired, the product $p_0 D$ must be increased.

Kinetic models [14] and Monte Carlo simulations [15] show that when the collision frequency becomes sufficiently small, the velocity of a given molecule in the expansion stops changing, simply because it encounters no further collisions. Beyond this point the distribution of molecular velocity components along the expansion axis ceases to evolve. The distribution of molecular velocities perpendicular to the expansion axis continues to narrow, however,

because molecules with large perpendicular components of velocity are driven off the axis by their own momentum. Thus, it becomes possible to define two translational temperatures, $T_\parallel$ and $T_\perp$. The parallel temperature component is related to the distribution of molecular speeds along the axis and stops evolving when the terminal Mach number is reached. The perpendicular temperature component continues to drop, however, purely as a result of geometrical effects.

2.3.3 Interaction with Background Gases

In any real apparatus the idealized continuum model will also break down when the expanding gas becomes sufficiently rarefied that its density approaches that of the background gases. At this point collisions between the background gases and the expanding gas cause the molecular velocity distribution to be randomized, so that the expansion becomes irreversible, leading to a serious increase in entropy. If the background gas density is high, the expansion travels through a shock zone in which the molecules are rapidly decelerated; if the background gas density is low, a molecule in the jet experiences a series of individual scattering events, and the randomization of the velocity distribution occurs over an extended region of space. The thickness of the shock zone thus depends on the density of the background gas.

For free expansion into vacuum, two types of shock zones develop. A barrel shock forms around the centerline of the expansion, resembling a paraboloid of revolution centered on the jet axis, opening from the expansion orifice. This ends at a second shock zone, called the Mach disk, which forms a nearly flat terminal shock wave perpendicular to the centerline of the beam. For high background gas densities these structures are well defined and are easily observed through Schlieren photography, as is shown in Figure 3 [16]. Within the volume defined by these limiting shock zones, the description of the jet offered earlier is quite adequate. This volume may then be further subdivided into a region where there are sufficient collisions to maintain equilibrium so that the continuum model is valid, followed by a region farther downstream where nearly collisionless flow occurs. This latter region has been termed "the zone of silence," in recognition of the fact that the speed of sound in the expanding gas [as given in Eq. (2.6)] has dropped to nearly zero, essentially eliminating the possibility of acoustic waves in the expanding gas flow. All of this comes to a crashing halt, however, when the expanding molecules reach the Mach disk and their velocities are randomized by collisions.

The location of the Mach disk depends only on the ratio between the source and background pressures, p_0 and p_B (and is independent of γ), although the thickness of the shock zone depends on the absolute magnitude of p_B [17]. If the location of the Mach disk is denoted by x_M, its position is correctly given by the

simple formula

$$x_M = 0.67\, D\sqrt{\frac{p_0}{p_B}}, \tag{2.14}$$

for values of the pressure ratio p_0/p_B in the range from 15 to 17,000 [12].

2.3.4 Seeded Beams

By adding a small mole fraction of a second species to the gas in the reservoir, one may create a seeded molecular beam. In the limit of high source density (high source pressure, p_0), the idealized continuum model of gas flow works well, and the behavior of the supersonic expansion is the same as that for a pure gas with molecular weight and heat capacity taken as the weighted average of the corresponding properties of the gases making up the mixture [9]. Under these high source pressure conditions, both component gases reach the same flow velocity and temperature at the same point in the expansion. For a gas mixture consisting of a low concentration of a heavy seed gas in a light carrier gas, the limiting flow velocity given by Eq. (2.3) is dominated by the more abundant, lighter gas, and it becomes possible to accelerate the seed gas to high kinetic energies. Furthermore, by virtue of the narrowing of the velocity distribution, these high kinetic energies are very well defined. As an example, by using a heated nozzle and a mixture of 0.1% xenon in hydrogen, xenon atoms have been accelerated to a kinetic energy of 30.2 ± 1.3 eV [18]. The ability to accelerate neutral species to such high, precisely defined energies has been quite useful in chemical dynamics investigations [19].

At low to intermediate source densities, the heavier gas molecules tend to lag behind the lighter gas molecules. In the expansion process, the heavier molecules are repetitively bombarded by the lighter gas molecules and are slowly accelerated to the full beam velocity. If the total source pressure is too low, however, less than complete acceleration is achieved, leading to "velocity slip" [9]. The phenomenon of velocity slip has been extensively investigated, both experimentally [20] and theoretically [21]. A simple model of seeded supersonic beams has been recently presented which provides useful expressions for terminal temperatures, velocity slip, enrichment factor, and beam intensity, and the validity of the model is documented by comparison to the properties of I_2 seeded in rare gas molecular beams [22].

A related effect observed in low- to intermediate-density seeded beams is a tendency of the heavy species to be concentrated on the jet axis. Multiple collisions with the lighter carrier gas during expansion tend to accelerate the component of velocity along the jet axis, but are less effective in modifying the perpendicular component of velocity. As a result, the initial trajectory of the

heavy particle is bent toward the jet axis, leading to an increase in concentration of the heavy species along the axis [23]. A theoretical analysis of the phenomenon has been proposed [24] and confirmed by experiment [25].

This concentration effect can be further enhanced by employing an annular nozzle to provide a sheath flow circumscribing the flow from a central orifice [26]. By seeding the carrier gas flowing from the central orifice with the molecule of interest, and providing a larger flow of pure carrier gas through the annular nozzle, gas dynamic focusing will drive the seed gas toward the centerline of the expansion. This has been shown to provide a factor of 30 increase in seed gas concentration on the centerline of the expansion [26]. This method is well adapted to interfacing capillary column gas chromatography to jet expansions, since the heavy analyte molecules are more easily detected if they are concentrated along the jet axis [27].

The primary advantages of seeded beams are that they allow the seed gas to be accelerated to the beam velocity of the carrier gas, and also allow the internal degrees of freedom of the seed gas to be cooled substantially, approaching the translational temperature achieved in the expansion. This latter aspect has been particularly useful for spectroscopic investigations, which are further considered later.

2.3.5 Skimmed Beams

Although many experiments such as those based on laser-induced fluorescence may conveniently be conducted in the free jet zone of silence, it is often advantageous to skim the free supersonic jet. This allows the supersonic beam to be collimated and transmitted into a second chamber which is operated at much lower pressure, a tremendous advantage for beam–surface or crossed-beam chemical dynamics experiments and for spectroscopic studies employing photoionization mass spectrometry for detection.

Two methods have been employed to skim the supersonic free jet and allow the transmission of a molecular beam into a second chamber. In the simplest [28], a low background pressure (10^{-3} to 10^{-4} torr) is maintained in the source chamber, preventing the formation of serious shock waves in front of the skimmer, which is typically conical in shape with a full angle of 25 to 30°. The skimmer is placed some distance from the back wall of the first chamber, so that there is little interference from gas molecules scattering off of the wall. The lack of significant shock waves allows the molecular beam to be passed into the second chamber without serious attenuation.

In the alternative method [29, 30], a relatively high background pressure (10^{-2} to 1 torr) is maintained in the source chamber, leading to a very pronounced barrel shock and Mach disk. A precisely manufactured skimmer is inserted into the free jet zone of silence, and the central core of the supersonic

expansion is transmitted into the second chamber. This leads to a well-defined system of shock waves attached to the skimmer. With careful skimmer design, however, no shock zone develops on the leading edge of the skimmer (which would impede the flow into the second chamber), and no shock waves are attached to the interior portion of the skimmer (which would disrupt the supersonic flow in the second chamber). The optimal skimmer design has been determined empirically [30] and has a full included internal angle of 45° and a full included external angle of 55°. The influence of skimmer length, diameter, and distance from the expansion orifice has been discussed [30]. Although the problem of skimmer interference in the high-pressure source has been solved, such sources seem to require extreme care for proper operation [26].

2.4 Clustering

From the very earliest investigations [31], clusters have been readily formed in supersonic expansions, and this has led to tremendous advances in our understanding of weakly bound cluster species. Clusters generated in supersonic molecular beams have now been investigated by microwave [32], infrared [33], and visible/ultraviolet spectroscopy [34]; they have even been structurally studied through electron diffraction methods [35]. Ionic clusters have also been studied using the techniques of supersonic expansions [36]. The production of clusters in a supersonic expansion also affords one of the cleanest methods of studying the initial steps in nucleation of a supersaturated vapor, chiefly because collisional processes in the jet are well understood [37].

Unlike translational cooling, which results from binary collisions, condensation of monomers to form clusters requires three-body collisions with the third body carrying off the energy. The total number of binary collisions occurring during the expansion is proportional to $p_0 D$ [38], and for this reason the terminal Mach number (a measure of the translational cooling) is a function of $p_0 D$, as given in Eq. (2.13). The total number of three-body collisions occurring during the expansion is proportional to $p_0^2 D$, while the mass throughput through the nozzle is proportional to $p_0 D^2$ [38]. Thus, the production of clusters will be maximized while maintaining a given gas throughput by increasing the reservoir pressure, p_0, and decreasing the nozzle diameter, D, to maintain a constant value of $p_0 D^2$.

A combined theoretical and experimental study of the influence of nozzle shape on cluster formation has been presented in which a sharp-edged orifice, a slightly converging "ideal" orifice, and a straight, capillary tube orifice were examined (see Figure 4) [39]. Although all three were calculated to give similar flow fields at large distances from the nozzle, the three differed significantly in their flow fields near the nozzle. As gas expands through an orifice, the gas flow

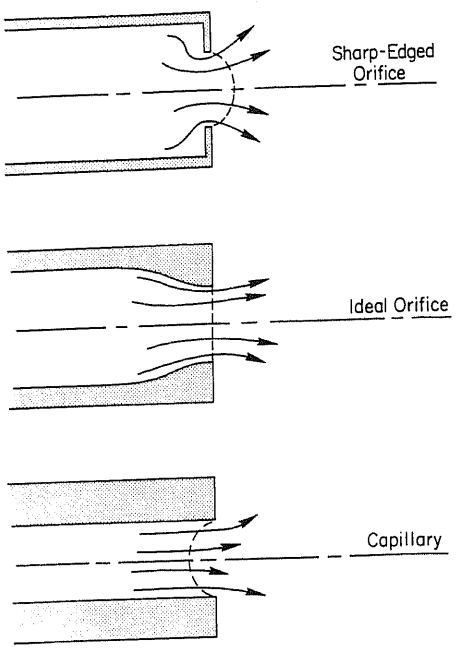

FIG. 4. Qualitative depiction of the streamlines and sonic surfaces for three types of nozzles shown in cross section. Reprinted with permission from H. R. Murphy and D. R. Miller, *J. Phys. Chem.* **88,** 4474 (1984). Copyright 1984, American Chemical Society.

velocity increases. The locus of points at which the flow velocity equals the local speed of sound is termed the "sonic surface," and it was in the shape and location of the sonic surface that the three nozzle types differed most significantly. The sharp-edged orifice led to a convex sonic surface located outside of the nozzle, the slightly converging "ideal" orifice led to a planar sonic surface at the end of the nozzle, and the straight, capillary nozzle led to a concave sonic surface located a short distance inside the capillary tube. The capillary nozzle was found to generate argon dimers in roughly twice the concentration of the other two nozzles, presumably because gas passes through the sonic surface earlier in the expansion in this design, thereby allowing greater cooling early in the expansions, before the gas density drops significantly.

Clustering can also be enhanced by confining the expansion after it passes through the sonic surface by the addition of a diverging section downstream of the nozzle throat [37]. This limits the expansion to a smaller angular range, thereby maintaining a high density during the initial portion of the expansion, which is most critical for the growth of clusters. A disadvantage is that a boundary layer develops on the inside of the diverging section, which tends to

limit the terminal Mach number and ultimate temperature achieved in the expansion [40].

Clustering of a condensible gas also proceeds more readily if it is diluted in an inert, noncondensible gas such as helium or neon [37]. Presumably, the helium or neon acts to thermalize the growing clusters, so that the sequential addition of monomers is not seriously hampered by the heat of condensation which is released in the process. Finally, the growth of clusters is considerably aided by the use of a slit nozzle geometry, for which the gas density drops linearly, rather than quadratically, with distance from the source. Three-body collisions are therefore much more frequent than in the axisymmetic jet, greatly enhancing the formation of clusters or van der Waals complexes [40].

2.5 Supersonic Expansions from Slit Nozzles (Plane Jets)

2.5.1 The Idealized Continuum Model

The idealized continuum model applied to axisymmetric jets in Section 1.3.1 can also be applied to the ideal slit expansion. The expansion orifice is taken to be a slit opening of width D and of length L. If $L \gg D$ and one is concerned about conditions at distances $x \ll L$ downstream, it is sufficient to consider a slit of infinite length. A supersonic slit expansion then ensues if $D \gg \lambda_0$, where λ_0 is again the mean free path in the reservoir.

In an idealized continuum slit supersonic expansion, it is still assumed that the gas flows without heat transfer to the walls and without viscosity, and an adiabatic, isentropic expansion is obtained. Thus, Eqs. (2.2)–(2.7) still obtain for gas expansion from a slit nozzle. The critical distinction between expansion from a circular orifice and from a slit nozzle is that in the latter case expansion occurs only in one transverse dimension.

The functional dependence of the Mach number achieved in a slit supersonic expansion as a function of the distance downstream, x, is given by [41]

$$M(x) = A_s\left(\frac{x - x_0}{D}\right)^{(\gamma-1)/2} - B_s\left(\frac{x - x_0}{D}\right)^{-(\gamma-1)/2}, \tag{2.15}$$

where A_s, B_s, and x_0/D are parameters depending on the ratio of heat capacities, γ. Specific values are provided in Table II. Using Eq. (2.15) in combination with

TABLE II. Values of Parameters Used in Eq. (2.15)

γ	x_0/D	A_s	B_s
1.66$\bar{6}$ (5/3)	−0.218	3.06	1.21
1.40 (7/5)	0.810	3.46	1.36
1.286 (9/7)	0.205	3.83	1.67

Eq. (2.7), asymptotic expressions for the temperature, pressure, and density ratios at a downstream distance x are obtained (subject to the constraint $D \ll x \ll L$):

$$\frac{T(x)}{T_0} = C_s\left(\frac{x - x_0}{D}\right)^{-(\gamma-1)};$$

$$\frac{p(x)}{p_0} = F_s\left(\frac{x - x_0}{D}\right)^{-\gamma}; \tag{2.16}$$

$$\frac{\rho(x)}{\rho_0} = G_s\left(\frac{x - x_0}{D}\right)^{-1},$$

where C_s, F_s, and G_s are constants determined from A_s and γ. Because in a slit nozzle gas expands in only one transverse dimension, $\rho(x)$ decreases as x^{-1}, not x^{-2} as is characteristic of an axisymmetric expansion. For this reason, the exponents of $[(x - x_0)/D]$ in Eqs. (2.16) are decreased by a factor of 2 as compared to Eqs. (2.9). The slower decrease in molecular density and temperature in a slit nozzle expansion provides much higher binary and three-body collision rates, which are of great utility in the production of clusters. The two- and three-body collision rates for hard sphere argon atoms emerging from a reservoir at $p_0 = 100$ torr, $T_0 = 300$ K through a circular orifice 1 mm in diameter vs. a slit nozzle 1 mm in width have been calculated [40] and are shown in Figure 5. Collisions persist to far greater downstream distances in a slit nozzle expansion. This also suggests that slit nozzle expansions should be more effective in cooling recalcitrant degrees of freedom [41].

Slit nozzle expansions offer important advantages in spectroscopic applications. By using a probe laser beam directed parallel to the slit axis, it is possible to obtain the long path length needed for direct absorption measurements [42]. Further, because the decrease in density with distance is not so rapid as in the axisymmetric jet, one gains in absorption strength because of increased density as well as path length. Finally, because the gas streamlines diverge only in the direction perpendicular to the slit axis, spectroscopic interrogation of the sample using radiation propagating parallel to the slit reduces the Doppler broadening substantially [43]. This has been particularly useful in pulsed slit-jet expansion infrared absorption studies of hydrogen bonded species such as $N_2 \cdot HF$ [44].

2.5.2 Transition to Axisymmetric Flow

Even if the idealized continuum model remains valid, the characteristics of any real slit expansion will depart from those given in Eqs. (2.15) and (2.16) at distances $x \approx L$, where there will be a gradual transition from a one-dimensional expansion to the two-dimensional expansion that characterizes an axisymmetric

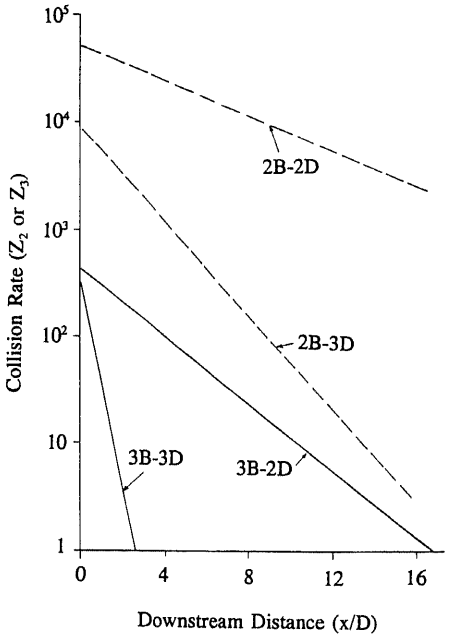

FIG. 5. Dependence of collision frequency on axial distance in an argon free jet expansion for source conditions of 100 torr and 300 K, and a nozzle diameter (or width, in the case of a slit expansion) of 1.0 mm. The two-body collision rates are indicated by dashed lines and the label "2B," three-body collision rates by solid lines and the label "3B." An axisymmetric jet is indicated by "3D," a wedge-shaped jet from an infinitely long slit nozzle by "2D." Reprinted, with permission, from reference [40].

jet. No complete treatment of the transition from plane to axisymmetric flow has yet been reported for the idealized continuum model. For large aspect ratios (L/D), the transition from plane to axisymmetric flow is expected quite far downstream, where the low collision rate may well make the assumptions of the idealized continuum model invalid. Such nonequilibrium effects have been investigated both theoretically and experimentally [45]. Unlike axisymmetric jets, where two translational temperatures ($T_{\|}$ and $T_{\perp}$) develop because of the loss of translational equilibration, slit nozzle expansions develop three distinct temperatures, associated with radial motion away from the source (T_r), motion along the long axis of the slit (T_z), and motion along the short axis of the slit (T_θ). At large distances these translational temperatures are such that $T_r > T_\theta > T_z$ [45].

2.5.3 Structure of Shock Waves in a Slit Nozzle Expansion

As discussed in Section 1.3.3, the shock wave structure of an axisymmetric jet is axisymmetric, consisting of a barrel shock and the Mach disk. Because of the

reduced symmetry of the slit nozzle expansion, the shock structure associated with a slit expansion is considerably more complex. In the limit of an infinitely long slit nozzle, however, the shock structure again retains the symmetry of the source. It consists of a barrel shock opening from the slit and a roughly planar Mach shock zone perpendicular to the expansion axis. The barrel shock is similar to the locus of points swept out by translating a parabola along the slit axis. The position, x_M, of the Mach shock in the limit of an infinitely long slit is given by

$$x_M = 1.23\, D\left(\frac{p_0}{p_B}\right)^{0.775} \tag{2.17}$$

for a slit expansion, where p_0 is the pressure in the reservoir, and p_B is the background pressure in the expansion chamber [46].

When a finite slit expansion ($L/D < \infty$) is employed (as is necessary in any real experiment), the shock structure is more complex, with lateral shock waves attached to the ends of the slit. These have been examined experimentally for high aspect ratio ($L/D = 450$ to 960) slits [46]. As the barrel shock opens up, the lateral shock waves close in, so that the aspect ratio of the shock structure initially mimics the ratio L/D of the slit, but decreases downstream. In certain p_0/p_B and L/D regimes, the expansion is still terminated by a Mach shock zone, but in other cases the expansion is terminated when the lateral shock waves approach one another and overlap before the Mach shock is encountered. For cases where the expansion is terminated by such overlap the downstream location, x_L, of the intersection (for aspect ratios $200 < L/D < 1000$ and pressure ratios $p_0/p_B < 5000$) is described by [46]

$$x_L = 40\, D\left(\frac{p_0}{p_B}\right)^{0.34}. \tag{2.18}$$

It is also observed that the location of the Mach shock for a source of finite aspect ratio departs significantly from that given in Eq. (2.17) [46].

2.6 Implementation and Applications

2.6.1 Pulsed Sources

As demonstrated by Eq. (2.13), achieving low temperatures (or high Mach numbers) in an axisymmetric jet requires large values of the pressure–diameter product, $p_0 D$. Since the mass throughput of the nozzle is proportional to $p_0 D^2$, pumping considerations will ultimately determine the cooling attainable for given nozzle diameter D. Similar considerations also apply to slit nozzles.

A practical solution is to employ pulsed supersonic expansions, thereby reducing the duty cycle (and the pumping requirements) considerably. Pulsed expansions are particularly useful for applications involving pulsed lasers.

A question that arises in the implementation of a pulsed nozzle design is how long the nozzle must remain open for a supersonic expansion to fully develop. This duration will ultimately limit the useful duty cycle of the pulsed valve. A useful rule of thumb is that the pulsed valve must be fully open for a time $\Delta t \geq 4D/a_0$ for a supersonic expansion to fully develop, where a_0 is the speed of sound in the reservoir, given by Eq. (2.6) [47]. Here "fully open" implies that the gas flow rate is limited by the throat diameter of the nozzle, instead of any constrictions around the valve mechanism. Indeed, if the gas flow is limited by constrictions associated with the valve mechanism, the system will never reach the fully developed supersonic flow expected for the nozzle diameter, even if it is operated continuously. For the rare gases helium, neon, and argon expanding through a 1 mm orifice, this inequality requires the nozzle be fully open for 4, 9, and 12 μs, respectively, for the full development of supersonic flow. Presently no mechanical design exists for a pulsed valve that can fully open and close in such a short time period, so it may be assumed that full supersonic flow is achieved in a pulsed valve, provided it is opened sufficiently that flow is limited by the nozzle throat diameter.

Numerous pulsed valve designs have been described, and some are even commercially available. An early design used a pulsed electromagnet to repel a diamagnetic diaphragm, thereby opening a seal and allowing gas to flow for a period of 350 μs [48]. Another approach now rarely employed involved the use of a sliding piston [49] or other sliding seal [50] (typically driven by a solenoid) to open a nozzle for a period of 1 to 3 ms. An alternative is to discharge a capacitor through a "hairpin" consisting of a fixed conductor and a spring, with the result that the induced magnetic fields cause the conductors to repel one another, opening a valve and allowing gas to flow for a period of 350 μs [51, 52]. This basic design, which is commercially available [53] and is illustrated in Figure 6, can produce pulses as short as 10 μs in duration [54]. This represents the shortest gas pulse ever created in the laboratory.

Piezoelectric crystals can also be used to open and close a pulsed valve, producing short pulses (100 μs to 10 ms in duration), with repetition rates to 750 Hz [55]. Such valves are now commercially available for researchers using pulsed supersonic beams [56].

Another approach in common use employs a solenoid to lift a poppet from a sealing surface, allowing gas to flow. After the current pulse to the solenoid is terminated, a spring closes the valve. One design has been developed for use to temperatures as high as 670 K [57], while others have used modified commercial fuel injector valves [58], one of which has produced pulses 600 μs in duration, with a prominent inital peak having a FWHM of 150 μs [59]. This modified solenoid-spring design is also commercially available [60].

A variant of this approach uses one solenoid coil to open the valve and a second to close it [61–63]. At least one such device has provided pulses as short

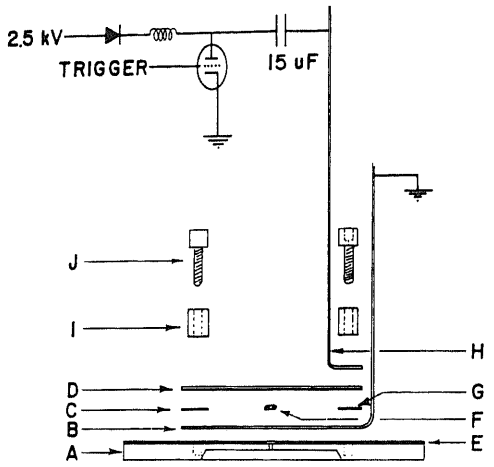

FIG. 6. An example of the "hairpin" pulsed valve, employing a stainless steel baseplate (A), a copper return conductor (B), a copper spacer (C), a copper-plate spring steel strip (D), an insulating coating of epoxy (E), a Viton O-ring (F), a Teflon spacer (G), a copper high-voltage input lead (H), plastic clamp bars (I), and a clamping screws (J). The nozzle is driven by discharging the capacitor charged to 25 kV through the elements H, D, C, and B, causing magnetic repulsion between the elements labeled B and D. This lifts element D off of the O-ring, allowing gas to flow. Reprinted, with permission, from reference [52].

as 10 μs in duration [64]. Details of such a valve are displayed in Figure 7. In most applications a spring is used to hold the valve closed when the solenoid currents are turned off.

Finally, two designs for pulsed slit expansions have been reported. One design uses two tight-fitting concentric cylinders with slits cut into them, which are rotated relative to one another. A gas pulse is emitted only during the short time that the slits are aligned providing a pulse duration of 150 μs [65]. Another design (shown in Figure 8) uses a solenoid to accelerate a plunger, which acts as a hammer, striking a rod connected to an elastomer seal over a slit orifice [66]. The impact causes the valve to open quickly, and a leaf spring is then used to close the valve, producing reproducible pulses 150–600 μs in duration.

With all of these designs now available, pulsed supersonic beam sources have become quite commonplace. Indeed, the maturity of pulsed supersonic expansion technology has enabled the focus of research to be shifted from technology development to applications.

2.6.2 Spectroscopic Applications

Spectroscopic applications of supersonic beams have become increasingly important since the pioneering experiments of Smalley, Levy, and Wharton first

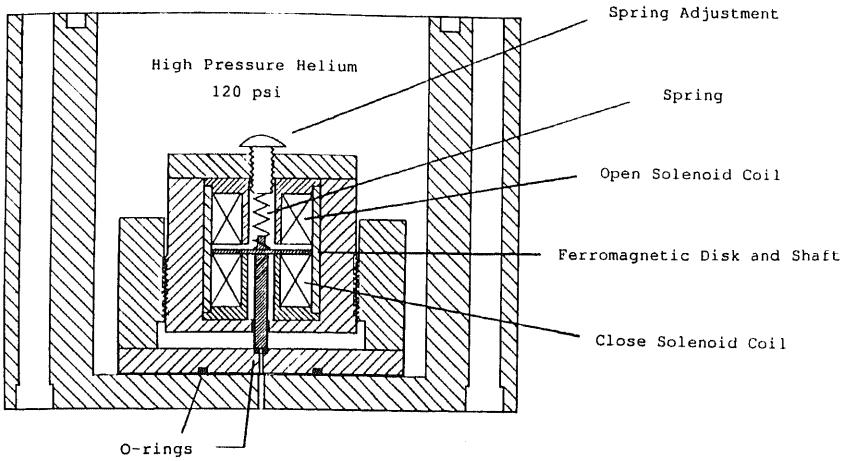

FIG. 7. An example of a double solenoid pulsed valve, in which a current is supplied to the *open* solenoid coil, which pulls the ferromagnetic disk and shaft up, allowing gas to flow through the small O-ring. A current through the *close* solenoid coil then pulls the ferromagnetic disk and shaft down, resealing the O-ring. A spring holds the valve closed when the solenoid currents are turned off. Reprinted, with permission, from reference [63].

established the advantages of the technique [67]. Since then, several reviews have been published concerning the application of supersonic jet spectroscopy to stable molecules, complexes, radicals, and ions [33, 34, 38; 68, 69]. The field of supersonic jet spectroscopy has become so vast that it is impossible to review it in a short article such as this. For this reason only the most promising techniques for the generation and study of jet-cooled clusters, radicals, and ions are considered, omitting stable species entirely.

The supersonic nozzle, particularly when operated in a pulsed mode, can be easily combined with other techniques for the generation and jet-cooling of reactive species, some of which are quite fragile. The earliest investigations of jet-cooled radicals involved species such as NaNe and NaAr, generated using a sodium oven as the reservoir in a supersonic expansion employing neon or argon [70]. Other radicals, such as CH_2 [71], CN [72], SH and S_2 [73], HCO [74], and allyl [75], were subsequently produced and cooled by laser photolysis in the high-pressure zone of a supersonic expansion, a method which is certain to remain productive well into the future.

Other methods for generating jet-cooled radicals and ions employ discharge techniques [76]. A particularly successful method for obtaining spectra with a high degree of rotational cooling uses a corona discharge near the exit orifice of a supersonic expansion, as schematically illustrated in Figure 9 [77, 78]. This

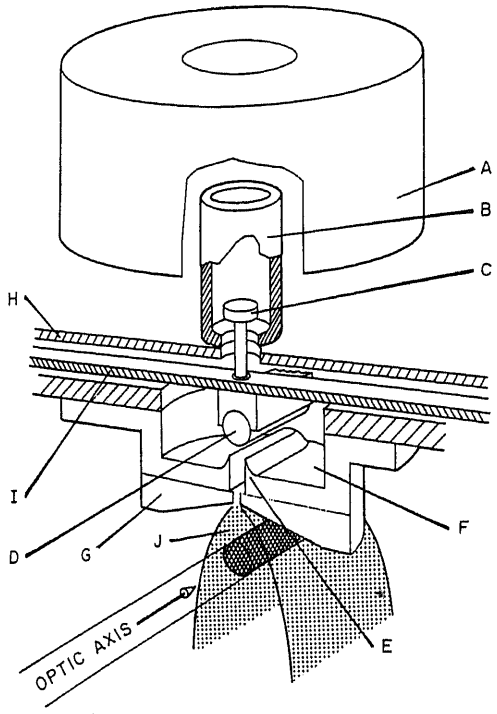

FIG. 8. Cutaway view of a slit pulsed valve. In operation, a current pulse through solenoid (A) accelerates plunger (B) against rod (C), which is connected to the seal assembly. The elastomer seal (D) is lifted from nozzle holder (E), permitting gas in plenum (F) to flow through interchangeable nozzles (G). The seal assembly continues upward until it hits stop (H). A leaf spring (I) returns the seal to the resting position, closing the valve. The resulting wedge-shaped expansion (J) provides a long path length, high-density sample at low (5–15 K) temperature. Reprinted, with permission, from reference [66].

method has been shown to be capable of producing fragile polyatomic radicals such as methyl nitrene (CH_3N:), which is produced in an excited electronic state. A continuous corona discharge source with a slit geometry has also been developed, providing reduced Doppler widths and narrowing the rotational linewidths [79]. A variant of the corona-excited discharge technology has also been applied to pulsed systems [80].

Another significant advance in the use of supersonic expansions to study radicals employs a flash pyrolysis source just prior to expansion into vacuum [81, 82]. In the initial application of this method, flash pyrolysis of *t*-butyl nitrite led to the production of jet-cooled methyl radicals with a rotational temperature of 40 K [83]. The technique has been used to record spectra of jet-cooled

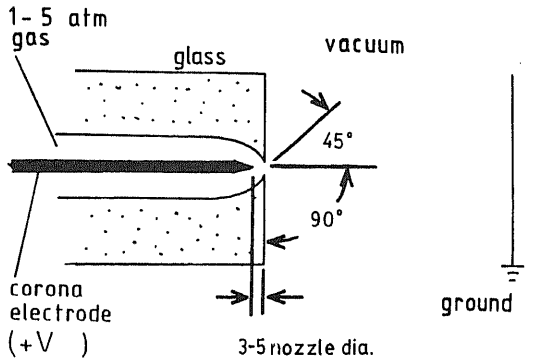

FIG. 9. Schematic diagram of a corona discharge nozzle, reprinted with permission from reference [78]. Important points are (1) the free expansion into a 90° half-angle on the low-pressure side, (2) the 45° half-angle of taper on the high-pressure side, and (3) the location of the corona electrode 3–5 nozzle diameters from the nozzle throat. The nozzle must be an electrical insulator, such as glass. Electrical continuity is formed by ionic conduction in the vacuum to the vacuum chamber.

propargyl [84], allyl [85], vinyl [86], CCl_2 [87], $SiCl_2$ [88], and $GeCl_2$ [89] radicals, along with formyl cyanide (HCOCN) [90] and cyclobutadiene [91]. A schematic drawing of a flash pyrolysis nozzle is shown in Figure 10. Again, it is clear that this technique will be widely used in the future.

Laser ablation of a target in the throat of a supersonic expansion has also become a common technique for generating jet-cooled metal and semiconductor clusters [92]. Several nozzle designs have been described, employing metal rods [62], disks [93], or wires [94]. In combination with laser-induced fluorescence or resonant two-photon ionization spectroscopy, this has become a powerful method for obtaining information on metal-based radicals such as metal dimers and trimers [95], metal diatomics MX [96], and larger clusters. This source has also been used for detailed studies of metal cluster reactivity [97] and bond strengths [98], and for production of carbon clusters for spectroscopic study [99]. Indeed, the soccer-ball structure of the famous C_{60} molecule, buckminsterfullerene, was first proposed to explain the anomalous intensity of the mass 720 peak in the mass spectrum generated by laser vaporization of graphite in a pulsed supersonic jet [100]. More recently, metal–carbon structures with the chemical formula of M_8C_{12} have been found to be particularly stable, and a dodecahedral structure has been proposed [101]. It is certain that the laser-vaporization supersonic expansion method will be a productive technique for the study of reactive chemical species for many years to come. A particular advantage of this method is that cations and anions are produced in the laser-induced plasma, and these are jet-cooled in the subsequent expansion into vacuum as well [102]. The

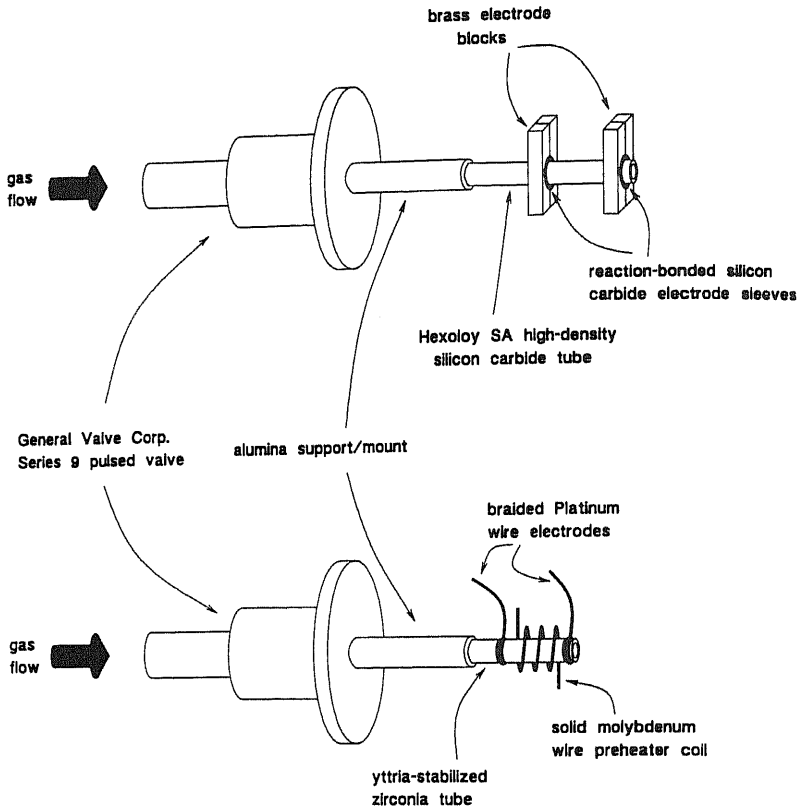

FIG. 10. Two pulsed pyrolysis nozzles used for the flash pyrolytic production of hydrocarbon radicals at temperatures up to 1800°C. The heated sections at the end of the extension tube are 1–2 cm long, corresponding to contact times with the hot zone of ≈10 μs for radical precursors seeded in helium carrier gas. Reprinted, with permission, from reference [82].

production of jet-cooled ions can be enhanced by directing excimer laser light into the nozzle source just prior to expansion [103].

In another interesting development, a collimated, 1 keV electron beam is used to ionize clusters produced in a supersonic expansion by crossing the supersonic cluster beam close to the expansion orifice [104]. Both positively and negatively charged clusters were generated, indicating that some clusters successfully captured the slow electrons which were detached by electron bombardment. In another experiment, an ultraviolet light source has been used to eject low-energy photoelectrons from a metal surface close to the expansion orifice of a supersonic expansion, allowing clusters to nucleate on the low energy electrons to produce

stable cluster anions of $(H_2O)_n^-$, $(NH_3)_n^-$, etc. [105]. Supersonic beams have also been crossed near the expansion orifice with the output beams of effusive ovens, allowing the high-temperature species effusing from the oven to be picked up and cooled in the supersonic expansion [106]. By using an expansion of water vapor in helium and a sodium oven, for example, it has been possible to produce the surprising adducts $Na(H_2O)_n$ [107]. With these examples of clever hybrids of supersonic expansions and other techniques, it seems our only limitation in the future uses of supersonic beams lies in our own imaginations.

Acknowledgments

I gratefully acknowledge support of my on-going research program, which uses supersonic beams extensively, by the National Science Foundation under Grant Number CHE-9215193 and by the Petroleum Research Fund, administered by the American Chemical Society.

References

1. Luo, F., McBane, G. C., Kim, G., Giese, C. F., and Gentry, W. R. (1993). *J. Chem. Phys.* **98,** 3564; Schollkopf, W., and Toennies, J. P. (1994). *Science* **266,** 1345.
2. Liu, B., and McLean, A. D. (1989). *J. Chem. Phys.* **91,** 2348; Vos, R. J., van Lenthe, J. H., and van Duijneveldt, F. B. (1990). *J. Chem. Phys.* **93,** 643; Tawa, G. J., Whitlock, P. A., Moscowitz, J. W., and Schmidt, K. W. (1991). *Int. J. Supercomput. Appl.* **5,** 57.
3. Ramsey, N. F. (1993). "Thermal Beam Sources," in *Methods of Experimental Physics: Atomic, Molecular, and Optical Physics*, Volume II, R. Hulet and F. B. Dunning (eds.). Academic Press, New York; Ramsey, N. F. (1990). *Molecular Beams*, Oxford University Press, Oxford, U.K.
4. See, for example, Gingerich, K. A. (1980). *Faraday Symp. Chem. Soc.* **14,** 109, and references therein.
5. See, for example, Liepmann, H. W., and Roshko, A. (1957). *Elements of Gasdynamics*, John Wiley & Sons, Inc., New York; or Zucrow, M. J., and Hoffman, J. D. (1976). *Gas Dynamics*, Vol. I, John Wiley & Sons, Inc., New York.
6. Kantrowitz, A., and Grey, J. (1951). *Rev. Sci. Instr.* **22,** 328.
7. Kistiakowsky, G. B., and Slichter, W. P. (1951). *Rev. Sci. Instr.* **22,** 333.
8. Becker, E. W., and Bier, K. (1954). *Z. Naturforsch.* **9A,** 975; Becker, E. W., and Henkes, W. (1956). *Z. Phys.* **146,** 320.
9. Anderson, J. B. (1974). "Molecular Beams from Nozzle Sources," in *Molecular Beams and Low Density Gasdynamics*, P. P. Wegener (ed.). Marcel Dekker, Inc., New York.
10. Anderson, J. B., and Fenn, J. B. (1965). *Phys. Fluids* **8,** 780.
11. Owen, P. L., and Thornhill, C. K. (1948). *Aeronaut. Res. Council, Great Britain, R & M*, 2616.
12. Ashkenas, H., and Sherman, F. S. (1966). In *Rarefied Gas Dynamics*, 4th Symposium, Vol. II, J. H. de Leeuw (ed.), p. 84. Academic Press, New York.
13. McClelland, G. M., Saenger, K. L., Valentini, J. J., and Herschbach, D. R. (1979). *J. Phys. Chem.* **83,** 947.
14. Hamel, B. B., and Willis, D. R. (1966). *Phys. Fluids* **9,** 829.

15. Bird, G. A. (1970). *AIAA J.* **8,** 1998.
16. Bier, K. and Hagena, O. (1966). In *Rarefied Gas Dynamics*, 4th Symposium, Vol. II, J. H. de Leeuw (ed.), p. 260. Academic Press, New York.
17. Bier, K., and Schmidt, B. (1961). *Z. Angew. Phys.* **13,** 34.
18. Campargue, R., Lebehot, A., Lemmonier, J. C., and Marette, D. (1980). *Rarefied Gas Dynamics*, 12th Symposium, S. S. Fisher (ed.). *Progress in Astronautics and Aeronautics*, **74,** Part 2, 823.
19. Parks, E. K., and Wexler, S. (1984). *J. Phys. Chem.* **88,** 4492; Russell, J. A., Hershberger, J. F., McAndrew, J. J., Cross, R. J., and Saunders, M. (1984). *J. Chem. Phys.* **88,** 4494.
20. Hagena, O., and Henkes, W. (1960). *Z. Naturforsch.* **15A,** 851; Abuaf, N., Anderson, J. B., Andres, R. P., Fenn, J. B., and Marsden, D. G. (1967). *Science* **155,** 997.
21. Anderson, J. B. (1967). *Entropie* **18,** 33.
22. DePaul, S., Pullman, D., and Friedrich, B. (1993). *J. Phys. Chem.* **97,** 2167.
23. Anderson, J. B. (1967). *Am. Inst. Chem. Eng.* **13,** 1188.
24. Sherman, F. S. (1965). *Phys. Fluids* **8,** 773.
25. Rothe, D. E. (1966). *Phys. Fluids* **9,** 1643.
26. Hayes, J. M. (1987). *Chem. Rev.* **87,** 745.
27. Stiller, S., and Johnston, M. V. (1987). *Anal. Chem.* **59,** 567.
28. Fenn, J. B., and Deckers, J. (1963). In *Rarefied Gas Dynamics*, 3rd Symposium, Vol. I, J. A. Laurmann (ed.), p. 497. Academic Press, New York; Fenn, J. B., and Anderson, J. B. (1966). *Rarefied Gas Dynamics*, 4th Symposium, Vol. II, J. H. de Leeuw (ed.). Academic Press, New York; Anderson, J. B., Andres, R. P., Fenn, J. B., and Maise, G. (1966). In *Rarefied Gas Dynamics*, 4th Symposium, Vol. II, J. H. de Leeuw (ed.). Academic Press, New York.
29. Campargue, R. (1964). *Rev. Sci. Instrum.* **35,** 111; Campargue, R. (1966). In *Rarefied Gas Dynamics*, 4th Symposium, Vol. II, J. H. de Leeuw (ed.). Academic Press, New York.
30. Campargue, R. (1984). *J. Phys. Chem.* **88,** 4466.
31. Becker, E. W., Bier, K., and Henkes, W. (1956). *Z. Physik* **146,** 333.
32. Legon, A. C. (1983). *Ann. Rev. Phys. Chem.* **34,** 275; Legon, A. C., and Millen, D. J. (1986). *Chem. Rev.* **86,** 635; also see *J. Chem. Phys.* **78,** 3483–3552 (Flygare memorial issue).
33. Nesbitt, D. J. (1988). *Chem. Rev.* **88,** 843.
34. Levy, D. H. (1980). *Ann. Rev. Phys. Chem.* **31,** 197; Levy, D. H. (1981). *Adv. Chem. Phys.* **47,** 323; Heaven, M. C. (1992). *Ann. Rev. Phys. Chem.* **43,** 283.
35. Bartell, L. S., and French, R. J. (1990). *Rev. Sci. Instrum.* **60,** 6468; Bartell, L. S., and French, R. J. (1989). *Z. Phys. D* **12,** 7; Bartell, L. S. (1986). *Chem. Rev.* **86,** 491.
36. Castleman, A. W., Jr., and Keesee, R. G. (1986). *Chem. Rev.* **83,** 589.
37. Hagena, O. F. (1974). "Cluster Beams from Nozzle Sources," in *Molecular Beams and Low Density Gasdynamics*, P. P. Wegener (ed.). Marcel Dekker, Inc. New York; Hagena, O. F. (1981). *Surf. Sci.* **106,** 101.
38. Smalley, R. E., Wharton, L., and Levy, D. H. (1977). *Accts. Chem. Res.* **10,** 139.
39. Murphy, H. R., and Miller, D. R. (1984). *J. Phys. Chem.* **88,** 4474.
40. Ryali, S. B., and Fenn, J. B. (1984). *Ber. Bunsenges. Phys. Chem.* **88,** 245.
41. Sulkes, M., Jouvet, C., and Rice, S. A. (1982). *Chem. Phys. Lett.* **87,** 515.
42. Amirav, A., Even, U., and Jortner, J. (1981). *Chem. Phys. Lett.* **83,** 1.

43. Veeken, K., and Reuss, J. (1985). *Appl. Phys. B* **38,** 117.
44. Lovejoy, C. M., and Nesbitt, D. J. (1987). *J. Chem. Phys.* **86,** 3151.
45. Beylich, A. E. (1981). In *Rarefied Gas Dynamics*, 12th Symposium, Vol. II, *Progress in Astronautics and Aeronautics* **74,** Sam S. Fisher (ed.), p. 710.
46. Dupeyrat, G. (1981). In *Rarefied Gas Dynamics*, 12th Symposium, Vol. II, *Progress in Astronautics and Aeronautics* **74,** Sam S. Fisher (ed.), p. 812.
47. Saenger, K. L. (1981). *J. Chem. Phys.* **75,** 2467; Saenger, K. L., and Fenn, J. B. (1983). *J. Chem. Phys.* **79,** 6043.
48. Kuswa, G., Stallings, C., and Stam, A. (1970). *Rev. Sci. Instrum.* **41,** 1362.
49. Inutake, M., and Kuriki, K. (1972). *Rev. Sci. Instrum.* **43,** 1670.
50. Riley, J. A., and Giese, C. F. (1970). *J. Chem. Phys.* **53,** 146; Watters, R. L., Jr., and Walters, J. P. (1977). *Rev. Sci. Instrum.* **48,** 643.
51. Inoue, N., and Uchida, T. (1968). *Rev. Sci. Instrum.* **39,** 1461.
52. Liverman, M. G., Beck, S. M., Monts, D. L., and Smalley, R. E. (1979). *J. Chem. Phys.* **70,** 192.
53. R. M. Jordan Company, 990 Golden Gate Terrace, Grass Valley, CA 95945.
54. Gentry, W. R., and Giese, C. F. (1978). *Rev. Sci. Instrum.* **49,** 595.
55. Auerbach, A., and McDiarmid, R. (1980). *Rev. Sci. Instrum.* **51,** 1273; Cross, J. B., and Valentini, J. J. (1982). *Rev. Sci. Instrum.* **53,** 38.
56. Lasertechnics, 5500 Wilshire Avenue NE, Albuquerque, NM 87113.
57. Köhler, K.-A. (1973). *Rev. Sci. Instrum.* **44,** 73.
58. Behlen, F. M., and Rice, S. A. (1981). *J. Chem. Phys.* **75,** 5672; Tusa, J., Sulkes, M., Rice, S. A., and Jouvet, C. (1982). *J. Chem. Phys.* **76,** 3513.
59. Otis, C. E., and Johnson, P. M. (1980). *Rev. Sci. Instrum.* **51,** 1128.
60. General Valve Corporation, 19 Gloria Lane, Fairfield, NJ 07004.
61. Adams, T. E., Rockney, B. H., Morrison, R. J. S., and Grant, E. R. (1981). *Rev. Sci. Instrum.* **52,** 1469.
62. Hopkins, J. B., Langridge-Smith, P. R. R., Morse, M. D., and Smalley, R. E. (1983). *J. Chem. Phys.* **78,** 1627.
63. Lemire, G. W. (1989). Ph.D. thesis, University of Utah, Salt Lake City, Utah.
64. Adriaens, M. R., Allison, W., and Feuerbacher, B. (1981). *J. Phys. E: Sci. Instrum.* **14,** 1375.
65. Amirav, A., Even, U., and Jortner, J. (1981). *Chem. Phys. Lett.* **83,** 1.
66. Lovejoy, C. M., and Nesbitt, D. J. (1987). *Rev. Sci. Instrum.* **58,** 807.
67. Smalley, R. E., Ramakrishna, B. L., Levy, D. H., and Wharton, L. (1974). *J. Chem. Phys.* **61,** 4363; Smalley, R. E., Wharton, L., and Levy, D. H. (1975). *J. Chem. Phys.* **63,** 4977.
68. Engelking, P. C. (1991). *Chem. Rev.* **91,** 399.
69. Foster, S. C., and Miller, T. A. (1989). *J. Phys. Chem.* **93,** 5986.
70. Ahmad-Bitar, R., Lapatovich, W. P., Pritchard, D. E., and Renhorn, I. (1977). *Phys. Rev. Lett.* **39,** 1657; Smalley, R. E., Auerbach, D. A., Fitch, P. S., Levy, D. H., and Wharton, L. (1977). *J. Chem. Phys.* **66,** 3778.
71. Monts, D. L., Dietz, T. G., Duncan, M. A., and Smalley, R. E. (1980). *Chem. Phys.* **45,** 133; Xie, W., Harkin, C., and Dai, H.-L. (1990). *J. Chem. Phys.* **93,** 4615.
72. Farthing, J. W., Fletcher, I. W., and Whitehead, J. C. (1983). *J. Phys. Chem.* **87,** 1663.
73. Heaven, M., Miller, T. A., and Bondybey, V. E. (1984). *J. Chem. Phys.* **80,** 51.
74. Song, X.-M., and Cool, T. A. (1992). *J. Chem. Phys.* **96,** 8664; Cool, T. A., and Song, X.-M. (1992). *J. Chem. Phys.* **96,** 8675.

75. Getty, J. D., Burmeister, M. J., Westre, S. G., and Kelly, P. B. (1991). *J. Am. Chem. Soc.* **113,** 801; Getty, J. D., Liu, X., and Kelly, P. B. (1992). *J. Phys. Chem.* **96,** 10155.
76. Searcy, J. Q. (1974). *Rev. Sci. Instrum.* **45,** 589; Leasure, E. L., Mueller, C. R., and Ridley, T. Y. (1975). *Rev. Sci. Instrum.* **46,** 635; Brutschy, B., and Haberland, H. (1977). *J. Phys. E* **10,** 90; Ganteför, G., Siekmann, H. R., Lutz, H. O., and Meiwes-Broer, K. H. (1990). *Chem. Phys. Lett.* **165,** 293.
77. Droege, A. T., and Engelking, P. C. (1983). *Chem. Phys. Lett.* **96,** 316; Carrick, P. G., and Engelking, P. C. (1984). *Chem. Phys. Lett.* **108,** 505.
78. Engelking, P. C. (1986). *Rev. Sci. Instrum.* **57,** 2274.
79. Brazier, C. R., Carrick, P. G., and Bernath, P. F. (1992). *J. Chem. Phys.* **96,** 919.
80. Sharpe, S., and Johnson, P. (1984). *Chem. Phys. Lett.* **107,** 35; Sharpe, S., and Johnson, P. (1986). *J. Mol. Spectrosc.* **116,** 247; Sharpe, S., and Johnson, P. (1986). *J. Chem. Phys.* **85,** 4943.
81. Dunlop, J. R., Karolczak, J., and Clouthier, D. J. (1988). *Chem. Phys. Lett.* **151,** 362.
82. Kohn, D. W., Clauberg, H., and Chen, P. (1992). *Rev. Sci. Instrum.* **63,** 4003.
83. Chen, P., Colson, S. D., Chupka, W. A., and Berson, J. A. (1986). *J. Phys. Chem.* **90,** 2319.
84. Minsek, D. W., and Chen, P. (1990). *J. Phys. Chem.* **94,** 8399.
85. Minsek, D. W., Blush, J. A., and Chen, P. (1992). *J. Phys. Chem.* **96,** 2025; Blush, J. A., Minsek, D. W., and Chen, P. (1992). *J. Phys. Chem.* **96,** 10150.
86. Blush, J. A., and Chen, P. (1992). *J. Phys. Chem.* **96,** 4138.
87. Clouthier, D. J., and Karolczak, J. (1991). *J. Chem. Phys.* **94,** 1.
88. Karolczak, J., and Clouthier, D. J. (1993). *Chem. Phys. Lett.* **201,** 409.
89. Karolczak, J., Zhuo, Q., and Clouthier, D. J. (1993). *J. Chem. Phys.* **98,** 60.
90. Karolczak, J., Clouthier, D. J., and Judge, R. H. (1991). *J. Mol. Spectrosc.* **147,** 61; Clouthier, D. J., Karolczak, J., Rae, J., Chan, W.-T., Goddard, J. D., and Judge, R. H. (1992). *J. Chem. Phys.* **97,** 1638.
91. Kohn, D. W., and Chen, P. (1993). *J. Am. Chem. Soc.* **115,** 2844.
92. Dietz, T. G., Duncan, M. A., Powers, D. E., and Smalley, R. E. (1981). *J. Chem. Phys.* **74,** 6511.
93. O'Brien, S. C., Liu, Y., Zhang, Q., Heath, J. R., Tittel, F. K., Curl, R. F., and Smalley, R. E. (1986). *J. Chem. Phys.* **84,** 4074.
94. Weidele, H., Frenzel, U., Leisner, T., and Kreisle, D. (1991). *Z. Phys. D* **20,** 411.
95. Morse, M. D. (1986). *Chem. Rev.* **86,** 1049; Morse, M. D. (1993). *Adv. Metal Semiconductor Clusters* **1,** 83.
96. Bourne, O. L., Humphries, M. R., Mitchell, S. A., and Hackett, P. A. (1986). *Opt. Commun.* **56,** 403; Simard, B., Mitchell, S. A., Humphries, M. R., and Hackett, P. A. (1988). *J. Mol. Spectrosc.* **129,** 186; Simard, B., Mitchell, S. A., Hendel, L. M., and Hackett, P. A. (1988). *Faraday Disc. Chem. Soc.* **86,** 163.
97. Bechthold, P. S., Parks, E. K., Weiller, B. H., Pobo, L. G., and Riley, S. J. (1990). *Z. f. Phys. Chem.* **169,** 101; Kaldor, A., Cox, D. M., and Zakin, M. R. (1988). *Adv. Chem. Phys.* **70,** 211.
98. Armentrout, P. B., Hales, D. A., and Lian, L. (1994). *Adv. Metal Semiconductor Clusters* **2,** 1.
99. Moazzen-Ahmadi, N., McKellar, A. R. W., and Amano, T. (1989). *J. Chem. Phys.* **91,** 2140; Heath, J. R., and Saykally, R. J. (1990). *J. Chem. Phys.* **93,** 8392; Heath,

J. R., Saykally, R. J. (1991). *J. Chem. Phys.* **94,** 3271; Arnold, D. W., Bradforth, S. E., Kitsopoulos, T. N., and Neumark, D. M. (1991). *J. Chem. Phys.* **95,** 8753.

100. Kroto, H. W., Heath, J. R., O'Brien, S. C., Curl, R. F., and Smalley, R. E. (1985). *Nature* **318,** 162.
101. Guo, B. C., Kerns, K. P., and Castleman, A. W., Jr. (1992). *Sciences* **255,** 1411; Chen, Z. Y., Walder, G. J., and Castleman, A. W., Jr. (1992). *J. Phys. Chem.* **96,** 9581; Castleman, A. W., Jr., Guo, B., and Wei, S. (1992). *Int. J. Mod. Phys. B* **6,** 3587.
102. Bloomfield, L., Geusic, M. E., Freeman, R., and Brown, W. L. (1985). *Chem. Phys. Lett.* **121,** 33; Liu, Y., Zhang, Q.-L., Tittel, F. K., Curl, R. F., and Smalley, R. E. (1986). *J. Chem. Phys.* **85,** 7434.
103. Zheng, L.-S., Brucat, P. J., Pettiette, C. L., Yang, S., and Smalley, R. E. (1985). *J. Chem. Phys.* **83,** 4273.
104. Johnson, M. A., Alexander, M. L., and Lineberger, W. C. (1984). *Chem. Phys. Lett.* **112,** 285; Posey, L. A., and Johnson, M. A. (1988). *J. Chem. Phys.* **89,** 4807.
105. Armbruster, M., Haberland, H., and Schindler, H.-G. (1981). *Phys. Rev. Lett.* **47,** 323; Haberland, H., Schindler, H.-G., and Worsnop, D. R. (1984). *Ber. Bunsenges. Phys. Chem.* **88,** 270; Haberland, H., Langosch, H., Schindler, H.-G., and Worsnop, D. R. (1984). *J. Phys. Chem.* **88,** 3903; Haberland, H., Ledewigt, C., Schindler, H.-G., and Worsnop, D. R. (1984). *J. Chem. Phys.* **81,** 3742.
106. Steimle, T. C., Fletcher, D. A., Jung, K. Y., and Scurlock, C. T. (1991). *Chem. Phys. Lett.* **184,** 379.
107. Schulz, C. P., Haugstätter, R., Tittes, H. U., and Hertel, I. V. (1986). *Phys. Rev. Lett.* **57,** 1703.